

# SIMULATION OF THE GAMMA-RAY FLUX OF ELECTROSPHERES AND STUDY OF ITS DETECTABILITY IN OUR GALAXY

Théo FRANCEZ (theo.francez@obspm.fr), Fabrice MOTTEZ, Guillaume VOISIN

LUTH Observatoire de Paris

PSL

Laboratoire Univers et Théorie (LUTH), Observatoire de Paris-PSL



## 1. Abstract

### Context.

Electrospheres are the environments of magnetized and rapidly rotating neutron stars acting like particle accelerators. With their central star slightly less energetic than the one of a pulsar, they do not host electron-positron pair creation processes. They consist of a low density plasma made of primary high energy particles emitting gamma-rays that have been extracted from the star by the electric field. Even if we do not know their number, they are expected to be numerous ( $\sim 10^9$ ) in our Galaxy, accounting for the short life of pulsars and of their progenitors, and the long life of neutron stars. The radiative energy flux emitted by the low density plasma is too low to be observed and no electrospheres have been observed individually up to now. However, due to their large number, they could generate a diffuse gamma-ray flux detectable with the FERMI-LAT telescope. On a theoretical side, numerical solutions of electrospheres have already been computed

but the study of their output radiation remained phenomenological.

### Aims.

We want to study the spectra of electrospheres and to deduce some observables for the FERMI-LAT telescope.

### Methods.

A recent code, Pulsar Aroma, computing self-consistent stationary solutions of plasma dynamics of electrospheres with the magnetic moment inclined with respect to the rotational axis of the star (Mottez, 2024), was adapted to solve the radiative transfer of ultra-relativistic particles emitting curvature radiation.

### Results.

The spectral features of electrospheres are quite different from pulsars. As expected, their much lower luminosity makes them hard to detect as point source by FERMI-LAT but we think they can contribute to a diffuse background or even to the Galactic centre excess (GCE) high-energy tail.

## 4. Simulated spectra

The spectra of electrospheres have a shape different than the one of pulsars. They have a principal component peaking between 10 and 100 GeV and sharply decreasing at 1 TeV (fig. 4 and 5) but also display a secondary component above the TeV for some lines of sight when the quantity scaling the electric field,  $\frac{2\pi B}{P}$ , is high enough (fig. 5). Such emission peaks and components are at higher energy than gamma-ray pulsars which usually peak at a few GeV. We suggest that they would probably be annihilated by positron-electron pair cas-

cares at higher plasma density which explains why pulsars spectra usually peak at a few GeV. Nonetheless we have to mention that curvature radiation was treated here in the classical regime while quantum regime and synchro-curvature radiation are actually more adapted (Voisin, 2017). This would have the effect of shifting a bit the spectra toward lower frequencies, albeit not much. Further investigations in the code are also needed to assess the significance of the secondary component above the TeV to constrain its shape.

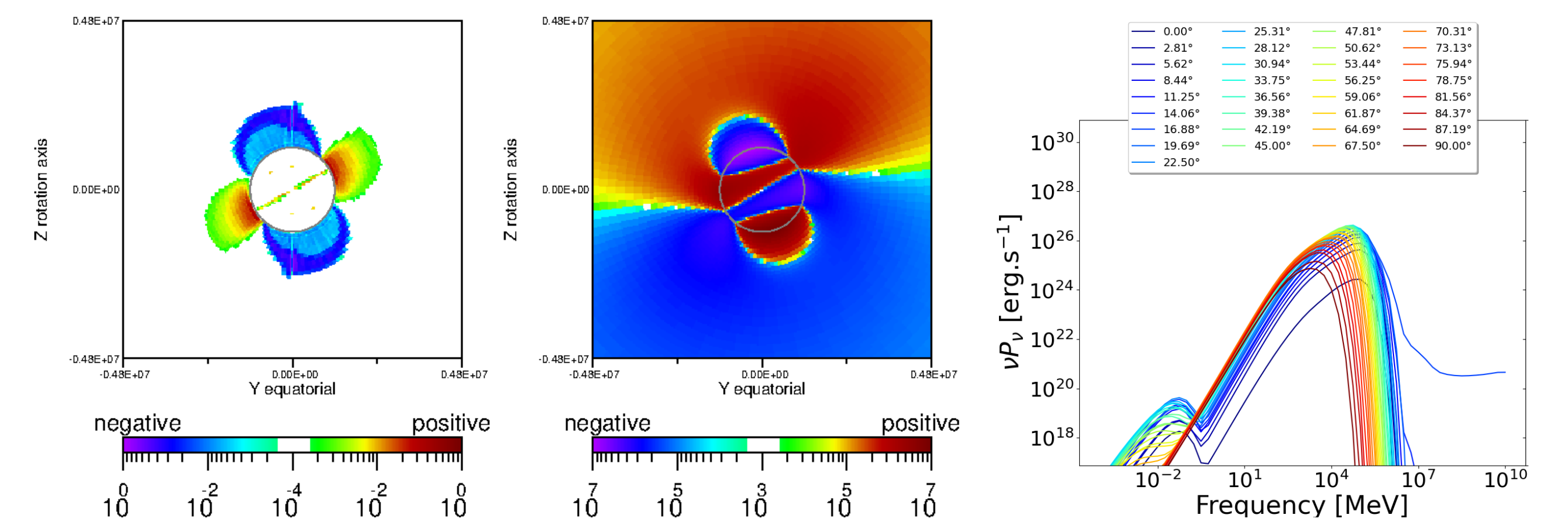


Fig. 4: Charge density (left, parallel electric field (center) and spectral energy density at different line of sight average over one period (right).  $B = 10^{11}$  G,  $P = 5$  s and  $i = 30^\circ$ .

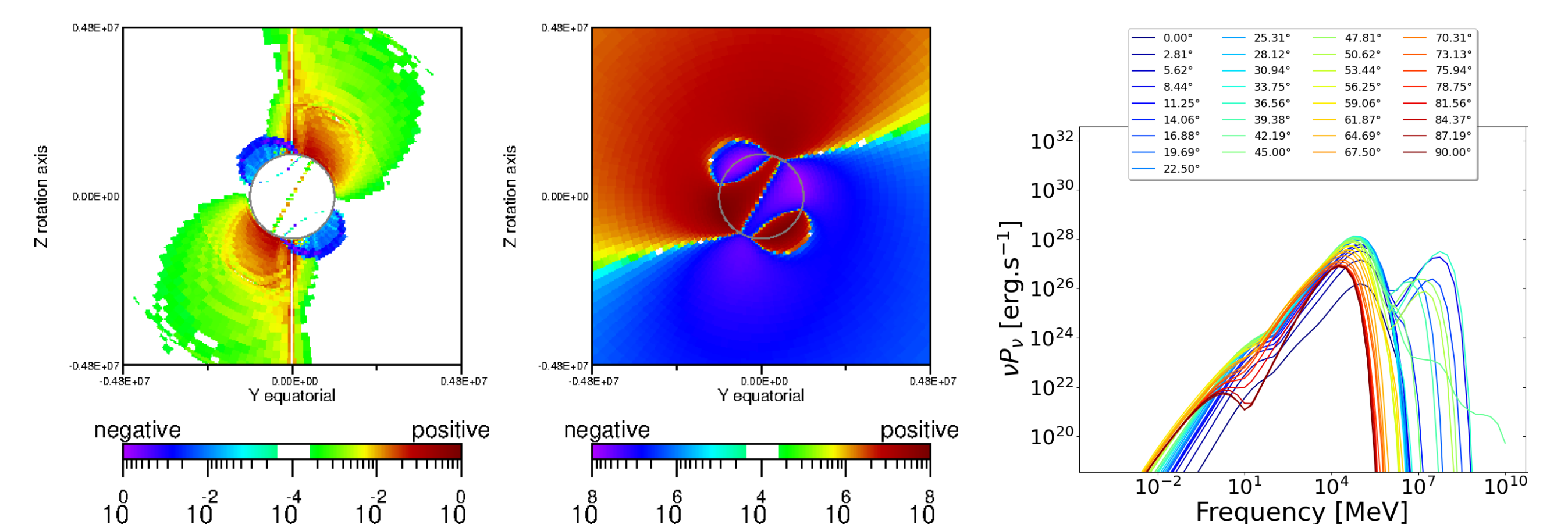


Fig. 5: Same as above but for  $B = 10^{12}$  G,  $P = 10$  s and  $i = 60^\circ$ .

## 2. Particle motion and electromagnetic fields

Pulsar Aroma combines iterative, PIC and Vlasov code methods to compute stationary self-consistent solutions of neutron star electrospheres. The iteration scheme of figure 1 is repeated until convergence.

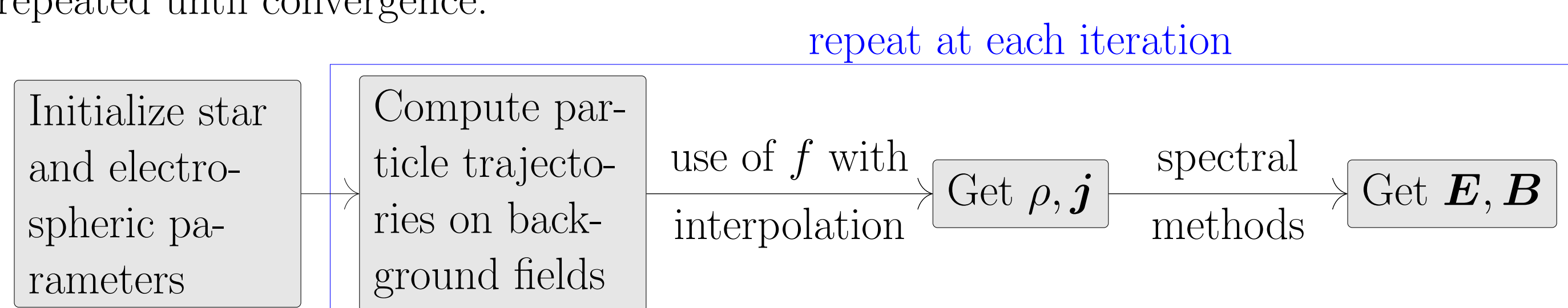


Fig. 1: Iteration scheme to compute a numerical solution of charge and current densities ( $\rho, \mathbf{j}$ ) and electromagnetic fields ( $\mathbf{E}, \mathbf{B}$ ).  $f$  is the distribution function of the particles.

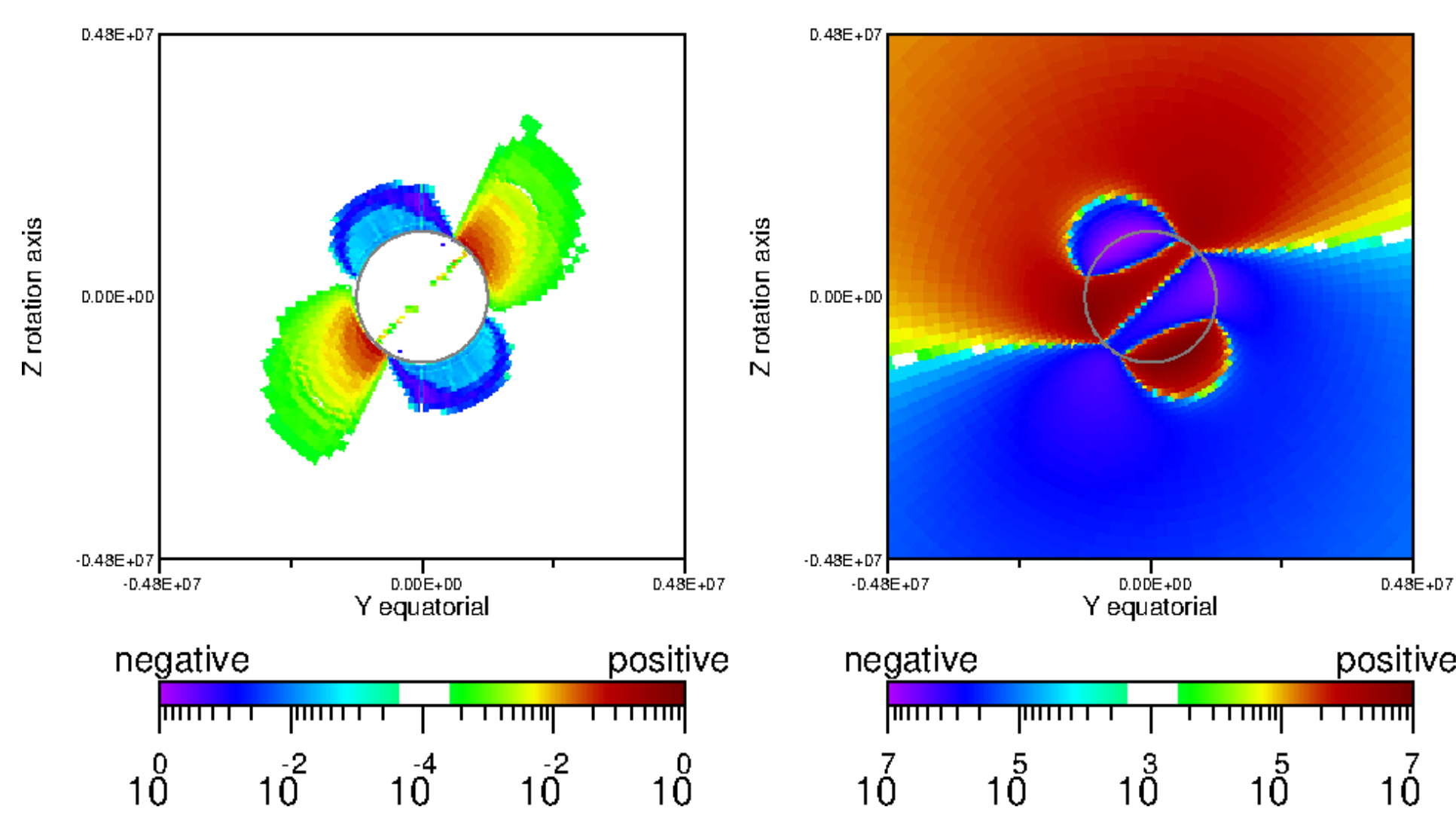


Fig. 2: Electrosphere with  $B = 10^{11}$  G,  $P = 5$  s and an inclination  $i = 45^\circ$  of the magnetic axis. Left: charge density. Right: Parallel (i.e. to the magnetic field) electric field.

## 3. Radiative processes at high energy

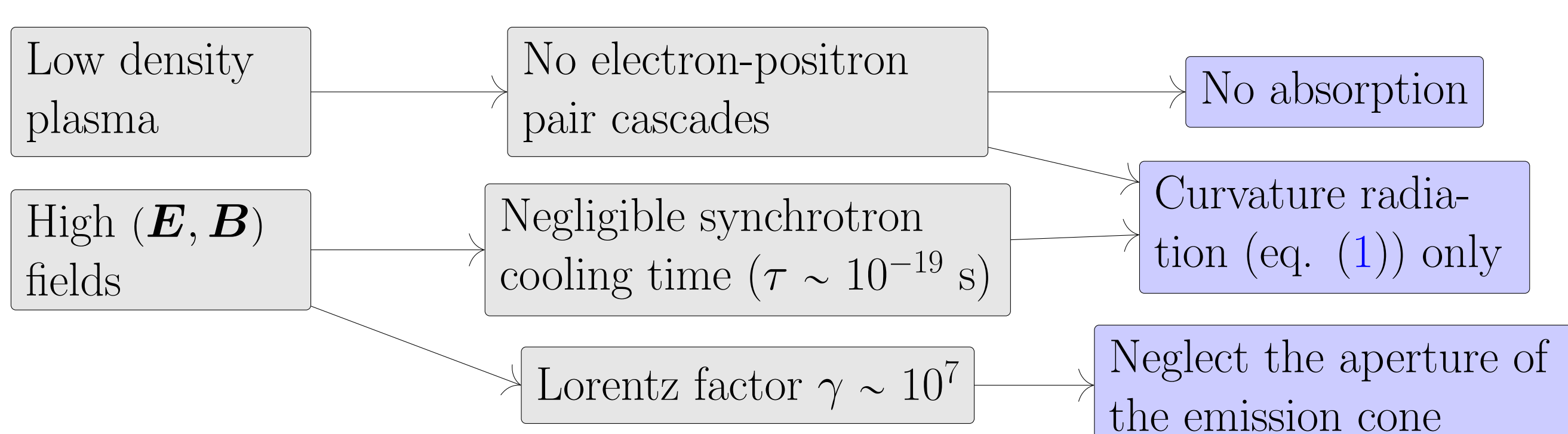


Fig. 3: Physical properties of electrospheres (light grey) and associated assumptions (light blue) for radiative processes.

The single particle spectrum (Rybicki, 1979) multiplied by the number of emitters  $N(\mathbf{r})$ , is

$$\mathcal{P}_\nu(\mathbf{r}) = \frac{\sqrt{3}q^2\gamma}{cT} F(x)N(\mathbf{r}) . \quad (1)$$

$F$  is a Westfold function and  $x = \frac{\nu}{\nu_c}$  with  $\nu_c$  the critical frequency.  $T = \frac{2\pi a}{c}$  is the period associated to the motion along the circle of radius  $a$ . In the iteration scheme of figure 1, the radiation emitted by particles is computed along their trajectories. Then, radiative maps are derived with interpolation similarly to the charge and current densities.

## 5. Observables

The total luminosities in the 0.1-100 GeV band (table 1) are  $10^4$  to  $10^6$  times lower than the typical gamma-ray luminosity of a pulsar in this band,  $L_\gamma \sim 10^{33}$  erg s $^{-1}$  (Smith et al., 2023). The typical FERMI-LAT sensitivity for the gamma flux in the 0.1-100 GeV band is  $F \sim 10^{-12}$  erg s $^{-1}$  cm $^{-2}$  so that for distances  $d \geq 0.01$  kpc we do not expect to observe any electrosphere.

B (G)	P (s)	i (°)	$L_\gamma$ (erg s $^{-1}$ )
$10^{10}$	1	30	$8.927 \times 10^{27}$
$10^{10}$	1	60	$5.192 \times 10^{27}$
$10^{11}$	5	30	$3.589 \times 10^{28}$
$10^{11}$	5	60	$1.936 \times 10^{28}$
$10^{12}$	10	30	$8.935 \times 10^{29}$
$10^{12}$	10	60	$9.042 \times 10^{29}$

Tab. 1: Luminosities of various electrospheres in the 0.1-100 GeV band averaged over one period.

However, the supposed large number of neutron star in our Galaxy, usually estimated as  $N \sim 10^9$ , is mainly composed of dead pulsars.

→ Estimated flux of  $N \sim 10^9$  electrospheres with an average gamma-ray luminosity  $L_\gamma \sim 10^{28}$  erg s $^{-1}$ , located at an average distance of 8.5 kpc:

$$F \sim 1 \times 10^{-9} \text{ erg s}^{-1} \text{ cm}^{-2} \text{ sr}^{-1} \approx 6 \times 10^{-7} \text{ GeV s}^{-1} \text{ cm}^{-2} \text{ sr}^{-1} .$$

⇒ Consequences:

1. plausible contribution to the diffuse gamma-ray background;
2. a contribution to the high energy tail (10-50 GeV) of GCE (e.g. Linden et al. (2016)) might also be worth the consideration because the spectrum peaks occur at the right energies (figures 4 and 5). However, it looks like we would need a bit more than  $10^9$  electrospheres otherwise the spectral energy  $\nu P_\nu$  seems too faint by a factor  $\lesssim 10$  to contribute significantly to it.

## References

- Linden T., Rodd N. L., Safdi B. R., Slatyer T. R.: High-energy tail of the galactic center gamma-ray excess. *Physical Review D* **94**(10), URL <http://dx.doi.org/10.1103/PhysRevD.94.103013> (2016)
- Mottez F.: Ab initio simulations of neutron stars' oblique electrospheres with realistic neutron star parameters. arXiv e-prints arXiv:2402.17348 (2024)
- Rybicki B. G.: Radiative processes in astrophysics. A Wiley-Interscience publication, J. Wiley and sons, New York Chichester Brisbane [etc. (1979)
- Smith D. A., Abdollahi S., Ajello M., et al.: The third fermi large area telescope catalog of gamma-ray pulsars. *The Astrophysical Journal* **958**(2), 191, URL <https://dx.doi.org/10.3847/1538-4357/acee67> (2023)
- Voisin G.: Numerical simulation of pulsar magnetospheres : detailed study of radiative processes. Theses, Université Paris sciences et lettres, URL <https://theses.hal.science/tel-01888379> (2017)